One-dimensional tungsten oxide nanostructures on Cu(110) surface

One-dimensional tungsten oxide nanostructures on Cu(110) surface

Romana Šedivá,[†,] Carolina Pistonesi,[‡] María E. Pronsato,[‡] Tomáš Duchoň,[†,§] Vitalii Stetsovych,[†,§§] Josef Mysliveček[†] and Karel Mašek[†]*

† Department of Surface and Plasma Science, Faculty of Mathematics and Physics, Charles University, V Holešovičkách 2, Prague 8, CZ-18000, Czech Republic

‡ IFISUR and Departamento de Física, Universidad Nacional del Sur, Avenida Alem 1253, Bahía Blanca, Argentina

KEYWORDS Tungsten oxide, model system, one-dimensional structures

ABSTRACT Thin epitaxial layers of tungsten oxide on metal substrates are suitable as model systems for investigation of chemical reactivity and catalytic properties. However, the ability to prepare epitaxial tungsten oxide model system in situ is quite rare. Here we present a method to prepare highly ordered tungsten oxide thin film on a Cu(110) single crystal substrate using physical vapor deposition in a reactive atmosphere of atomic oxygen. The oxygen induced reconstruction of the copper substrate gives rise to unique self-organized one-dimensional structures of tungsten oxide parallel with the Cu[1-10] crystallographic direction. Utilizing a combination of photoemission spectroscopy and density functional theory calculations we reveal emergent physicochemical properties related to the low-dimensionality of the system.

Specifically, we observe a support mediated charge redistribution at the interface and a momentum dependent modulation of the valence-band electronic structure. The unusual character of the one-dimensional oxide nanostructures on Cu(110) surface opens up a unique avenue for preparation of tungsten oxide-based functionalized nanostructures and provides options for further investigation of the fundamental properties of tungsten oxide.

Introduction

One-dimensional nanostructures with high surface to volume ratio can exhibit unique physicochemical properties compared with their bulk counterparts [1] and provide an intriguing field of research [2,3]. In particular, low-dimensional oxides on metal substrates have been extensively studied, revealing novel structural properties, electronic and magnetic behavior and also enhanced chemical reactivity [4,5]. Apart from the reduced dimensionality, another important feature of oxide nanostructures supported on metallic substrates is the proximity of the oxide-metal interface, which can significantly influence their electronic structure and catalytic performance. Accordingly, low-dimensional oxide systems are valuable for innovative model studies in the fields of heterogeneous catalysis and gas sensing.

Tungsten oxide is widely used in industrial processes as a catalyst and a sensor both in the pure form and doped by different metals [6–8]. The microstructure of reducible tungsten oxide can have a significant influence on its physicochemical properties. In non-stoichiometric tungsten, oxide W^{6+} ions are reduced to W^{5+} or W^{4+} ions through the formation of oxygen vacancies. These may serve as active sites for adsorption and determine selective catalytic processes taking place on the surface [9]. Vacancies alone or species adsorbed from reaction atmosphere also influence conductivity of the oxide [10,11].

Formation of tungsten oxide nanowires was reported on a mica substrate due to interaction with potassium atoms in the surface layer [12,13]. However, this system is not suitable for model studies due to mica's insulating properties severly restricting applicable surface science methods. Other forms of low-dimensional tungsten oxide nanostructures have been prepared [14,15], including a highly ordered monolayer of ternary tungsten oxide $CuWO_4$ grown on the (110) plane of a copper single crystal [16]. The low-index Cu(110) surface is known for its ability to reorganize easily upon adsorption of different species, minimizing its energy in the presence of the adsorbates. This process is typically related to sufficient mobility of surface atoms, which is thermally activated. The reorganization of the surface can result in the formation of new crystallographic facets [17,18] or monoatomic steps, possibly leading to periodic modulation of the copper-adsorbate interface [19–21].

Theoretical methods provide powerful complementary tools for understanding physical and chemical properties of nanostructured materials at an atomic level of detail. The few existing density functional theory studies concerning tungsten oxide nanowires point to a strong influence of the surface structure on the electronic density of states, the band structure and the band gap width [22,23]. Theoretical studies also confirm the generally expected effect of oxygen vacancies in tungsten oxide nanowires on the interaction with adsorbates, specifically NO_2 [24].

Experimental details and computational methods

The experiments took place in the Surface Science Laboratory in Prague. The tungsten oxide layers were prepared on the surface of a Cu(110) single crystal supplied by MaTecK, with a declared miscut less than 0.1 °. The crystal was cleaned by cycles of Ar^+ ion bombardment and annealing up to 600 °C under ultra-high vacuum (UHV) conditions. A thin tungsten oxide layer was deposited onto the clean Cu (110) surface at 400 °C by evaporation of tungsten trioxide

powder from an electron-heated evaporation source. The evaporation source allowed for deposition of very clean material at low deposition rate (2 Å/min) necessary for the formation of epitaxial layers. The deposition was carried out in a flux of reactive atomic oxygen produced by thermal gas cracker (TC50) in order to prevent excessive reduction of the vaporized tungsten trioxide. Oxygen partial pressure was maintained at $5 \cdot 10^{-5}$ Pa during the deposition. The thickness of the layer was 0.74 nm. It was determined via the attenuation of the Cu 2p signal of the substrate measured by X-ray photoelectron spectroscopy (XPS), assuming a homogeneous layer and disregarding elastic scattering. The inelastic mean free path of electrons in tungsten trioxide used in the calculation was d = 11.41 Å, as obtained from the TPP-2M formula [25].

Reflection high energy electron diffraction (RHEED), low energy electron diffraction (LEED) and scanning tunneling microscopy (STM) were used to investigate the surface structure. The chemical state and the electronic structure of the system were probed by means of X-ray photoelectron spectroscopy and angle-resolved photoelectron spectroscopy (ARPES). The samples were prepared and characterized in situ in the apparatus combining RHEED and XPS methods. For characterization by STM, LEED and ARPES the samples were transferred through the ambient air and recovered by annealing to 400 °C in $5 \cdot 10^{-5}$ Pa of oxygen. This procedure was carefully tested in order to make sure that it does not influence the structural and electronic properties of the samples. Theoretical models were proposed based on density functional theory (DFT) calculations addressing the geometry, the electronic structure and the electric charges of the system.

X-ray photoelectron spectroscopy of W 4f, O 1s and Cu 2p core levels was performed using X-ray radiation with energy of 1486.6 eV (Al K_α). ARPES measurements were conducted with He lamp providing radiation with energy of 21.2 eV (He I). Deconvolution of obtained data was

performed using W 4f 5/2 and W 4f 7/2 doublet with a spin-orbit splitting of 2.15 eV. Spectral lines were represented by pseudo-Voigt functions and a Shirley-type background was subtracted from the spectra. STM of the tungsten oxide layers was performed using chemically etched tungsten tips annealed in vacuum. The images were obtained probing occupied states of the sample. DFT calculations were performed using the Vienna Ab-Initio Simulation Package (VASP) [26–28], which employs a plane-wave basis set and a periodic supercell method. Potentials within the projector augmented wave (PAW) method [29] and the gradient-corrected functionals in the form of the generalized-gradient approximation (GGA) with the Perdew-Burke-Ernzerhof (PBE) functional [30,31] were applied. We used 6-8 ML thick slabs of sufficient lateral dimensions to accommodate the 6x2 reconstruction of the Cu surface and the deposited tungsten oxide species. During optimization, the first two surface layers and deposited species were allowed to relax, until a convergence of 1.0 meV for the total energy was reached. In all cases, a set of 3×3×1 Monkhorst-Pack k-points was used to sample the Brillouin zone. Density of states (DOS) curves were used to analyze the electronic structure of the system and the electronic charges of atoms were computed using Bader analysis [32]. Simulated STM images based on the DFT calculated charge density were used for evaluation of the models' accuracy.

Results and discussion

Well-defined thin layers of tungsten oxide were prepared by thermal evaporation of WO_3 powder in reactive atmosphere of atomic oxygen. The Cu(110) single crystal substrate was kept at 400 °C during the growth. Due to the combination of the elevated temperature and the exposure to atomic oxygen the copper substrate exhibited an oxygen induced Cu(110)–c(6×2)-O surface reconstruction [33].

Electron diffraction indicates one-dimensional character of the obtained tungsten oxide structures. We observe a set of uniformly spaced parallel planes in reciprocal space. According to the kinematic diffraction theory [34] such diffraction pattern is characteristic for a set of parallel one-dimensional wires in the real space, which are perpendicular to the reciprocal planes and, in our case, parallel to the Cu[1-10] crystallographic direction. The distance between the reciprocal planes is given by a regular spacing of the scatterers along the wires. The observed RHEED and LEED patterns are shown in Fig. 1. We recognize two sets of diffraction maxima at different intensity levels belonging to the tungsten oxide structures. No spots or lines of the copper surface are visible. The more intense maxima reflect the distance between the scatterers of (3.83 ± 0.01) Å. This distance is equal to the lattice parameter of tungsten oxide in the pseudo-cubic phase [35]. The less intense lines in between the stronger ones refer to a superstructure with double periodicity.

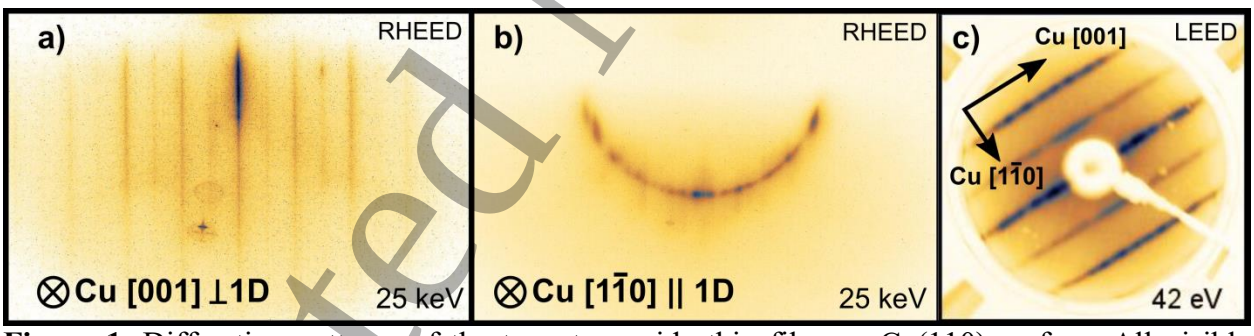

Figure 1. Diffraction patterns of the tungsten oxide thin film on Cu(110) surface. All visible patterns originate from the tungsten oxide overlayer, no diffraction spots or lines of the copper substrate are visible: (a) RHEED pattern in the direction perpendicular to 1D structures and (b) RHEED pattern in the parallel direction, both taken at primary energy E_p = 25 keV; (c) LEED pattern (E_p = 42 eV).

STM results confirm the appearance of parallel one-dimensional structures on the surface. Fig. 2(a) shows an overview STM image revealing structures prolonged in the Cu[1-10] direction and high steps perpendicular to the structures. The height of the steps is up to 3 nm according to the height profile in Fig. 2(b). The step height corresponds neither to the thickness of the deposited layer (0.74 nm) nor to the height of a monolayer step on the Cu(110) surface (1.28 Å). We presume that the copper surface rearranged itself due to interaction with the tungsten oxide overlayer. The schematic of the rearrangement is shown in Fig. 2(c). Considering the geometry of the problem we can determine that the newly established high steps are formed by Cu(1-10) facets, which are equivalent to the Cu(110) surface. In a high-resolution STM image (Fig. 2(d)) we can identify two different types of one-dimensional structures that are present on the Cu(110) terraces between the high steps. The difference between the structures becomes apparent when looking at averaged height profiles taken along the Cu[1-10] direction (Fig. 2(g)). Both profiles are modulated with the main period equal to the distance of 3.83 Å, which corresponds to the more intense lines in the diffraction patterns. However, one of the structures exhibits a significantly deeper minimum every second period, which corresponds to the characteristic length of 7.66 Å and therefore to the less intense maxima in the diffraction patterns. Structural elements of the LEED pattern of the sample (Fig. 1(c)) are fully replicated in the 2D fast Fourier transform of the STM image (Fig. 2(e)). To examine both structures further we also took averaged height profiles along Cu[001] direction perpendicular to the one-dimensional structures. Profiles taken in the areas with double periodicity (Fig. 2(h)) incorporate comparable features. Also height profiles from areas with single periodicity (Fig. 2(i)) contain similar sections in a particular order. However, without further analysis we cannot unambiguously determine the actual lateral size of the tungsten oxide one-dimensional structures.

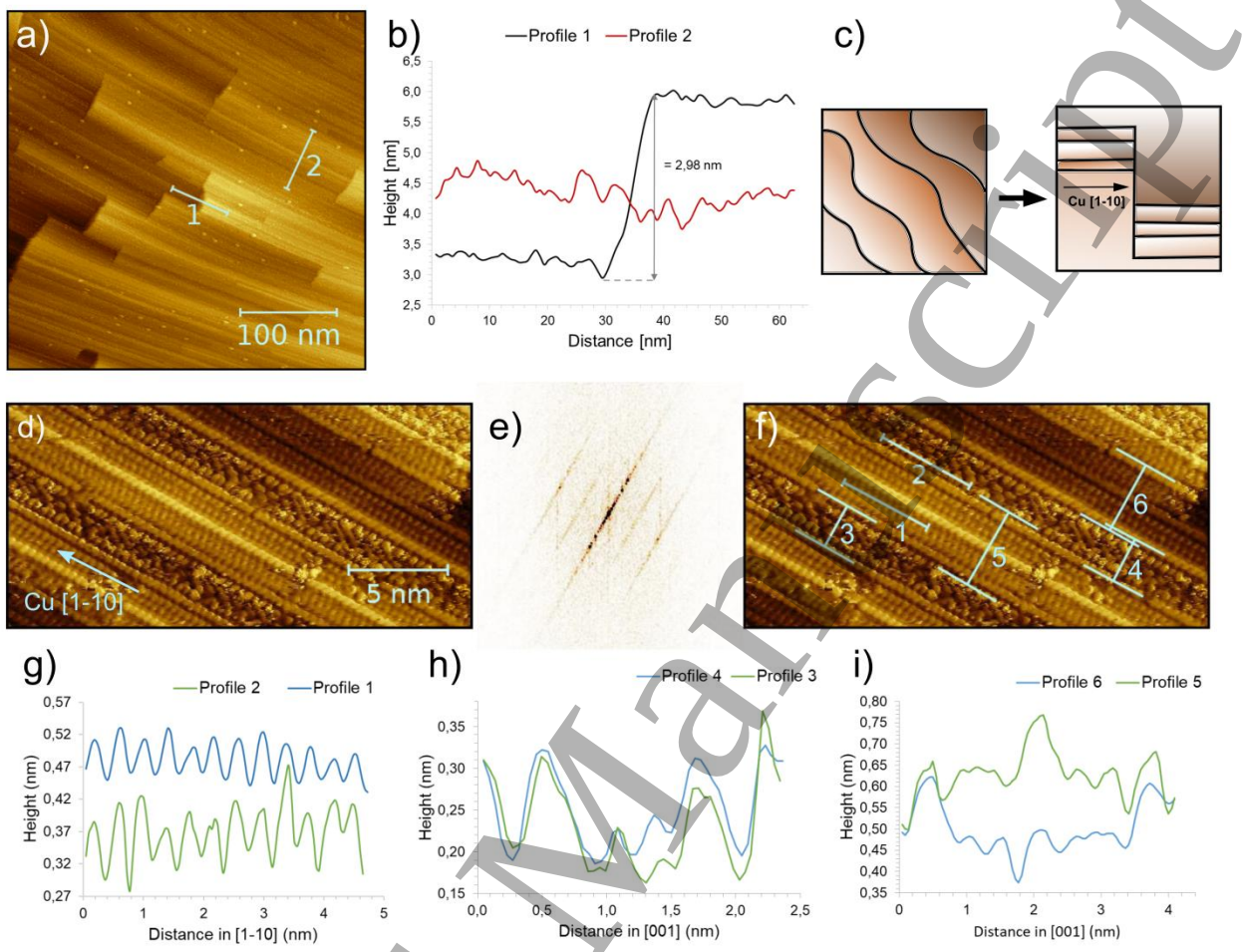

Figure 2. (a) Overview STM image of the WO_3/Cu(110) system showing reorganization of the copper surface steps. (b) Height profiles taken from (a). (c) Schematic representation of the reorganization of the copper surface due to the presence of tungsten oxide thin film. (d) Detailed STM image of the tungsten oxide nanowires. (e) 2D Fast Fourier Transform (FFT) of the panel (d), reproducing the LEED pattern in Figure 1(c). (f) Areas of origin of height profiles shown in the following panels. (g) Averaged profiles (width 10 px) taken along Cu [1-10] direction. (h) and (i) Averaged profiles (width 74 px) taken along Cu [001] direction.

According to the X-ray photoelectron spectrum shown in Fig. 3 the film stoichiometry corresponds to tungsten trioxide. The W 4f doublet is positioned at 34.9 eV with spin-orbit splitting of 2.15 eV and intensity ratio of 0.75. As is typical for oxides, it is located at higher

binding energy compared with the original metallic state, but its position is slightly shifted to a lower binding energy than what is usually reported for the W^{6+} state of the bulk material [36].

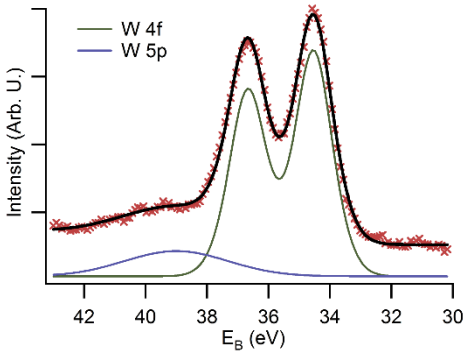

Figure 3. X-ray photoelectron spectrum of W 4f core emission line.

Reduced dimensionality of the prepared tungsten oxide structures is expected to give rise to perturbations of their electronic structure. In order to confirm the effect we have followed the valence band dispersion in directions parallel and perpendicular to the Cu [1-10] by ARPES. The results are shown in Fig. 4. We observed a disparity in the character of the valence band in the two directions. While a clear dispersing feature can be identified in the direction parallel to Cu[1-10], all bands are completely flat in the perpendicular direction. The lack of dispersion in the direction perpendicular to the Cu[1-10] is a footprint of the 1D character of the electronic states of the tungsten oxide [3], allowing us to refer to the observed structure as nanowires both structurally and electronically. Consequently, the reduced dimensionality of the electronic structure implies that the interwire electronic coupling is so weak that it is essentially masked by the intrinsic line width.

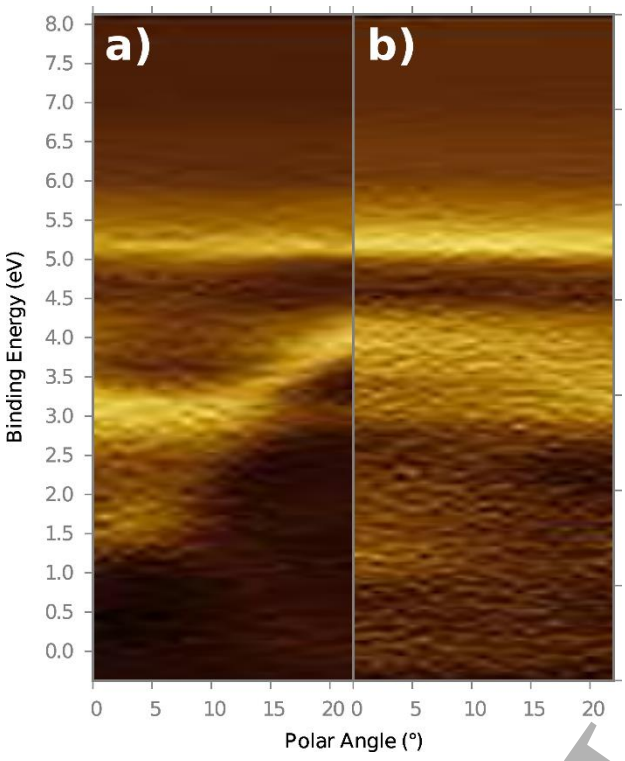

Figure 4. Angle resolved photoemission spectroscopy showing band structure of tungsten oxide nanowires measured along Cu[1-10] direction (a) and Cu[001] direction (b), which are directions parallel and perpendicular with respect to the nanowires, respectively. Measurements were performed at the photon energy of 21.2 eV. Visibility of the bands is enhanced by the first derivative over energy.

In order to learn more about the structures and epitaxy of the tungsten oxide nanowires on Cu(110) surface two theoretical models were considered - a nanowire composed of one line of tungsten oxide octahedrons (one line model) and a nanowire composed of two lines of tungsten oxide octahedrons (two line model), both supported on a Cu(110)-c(6x2)-O reconstructed surface [33] and oriented along Cu[1-10] direction. For the one line model, the copper surface was modelled by an eight layers slab with a lateral size of 6x2 the Cu(110) surface unit cell. It resulted in a supercell of about 7.3 Å by 15.4 Å and around 10 Å thick, including the eight oxygen atoms and two copper adatoms on the surface. The vacuum spacing between two

repeated slabs was 10 Å. For the two lines model we used a six layers slab with a lateral size of 6x4 the Cu(110) surface unit cell, resulting in a supercell of about 14.6 Å by 15.4 Å with thickness of 7.2 Å, including 16 oxygen atoms and 4 copper adatoms belonging to the Cu(110)-c(6×2)-O reconstruction.

The resulting equilibrium configurations for both models are shown in Fig. 5. Tungsten atoms are bonded on top of the oxygen atoms belonging to the Cu(110)-c(6×2)-O reconstruction. Each tungsten atom is coordinated by six oxygen atoms, forming a tungsten oxide octahedron - the standard building block of tungsten oxide [37,38]. Oxygen atoms of the Cu-(110)-c(6×2)-O reconstruction are part of the octahedrons, forming their bottom apex (below W atom, marked O_{below} in Fig 5). Further oxygen atoms on the apices of the octahedrons are marked $O_{aligned}$ - forming the W-O-W-O chain along Cu[1-10] direction, $O_{lateral}$ - bonded to the sides of W atoms and O_{above} - bonded on top of the W atoms (Fig. 5). The W-O-W-O chains along Cu[1-10] direction exhibit a zigzag lateral distortion, more pronounced for the one line model than for the two lines model. Thus, the distance between the tungsten atoms is on average 3.84 Å for the two lines model and 3.91 Å for the one line model. The lateral displacement of tungsten atoms perpendicular to the Cu[1-10] direction is approximately 0.17 Å for the one line model versus 0.07 Å for the two lines model. The average width of the wire is 3.39 Å and 7.04 Å for the one and the two lines models, respectively, while their heights are 4.32 Å and 4.54 Å.

The distance between the W atoms along Cu[1-10] direction corresponds to the main diffraction lines in the RHEED and LEED patterns (Fig. 1). The lateral distortions of the W-O-W-O chains represent a plausible source of the observed diffraction maxima belonging to the surface structure with double periodicity. Considering that the lateral distortions are more

prominent in the case of one line model, we propose that the structure with double periodicity represents an early stage of the nanowire´s growth, which corresponds to the one line model.

Electronic charges of the atoms were computed by Bader analysis and they are comparable for both models. In the case of the one line model the tungsten atoms present an average charge of 4.427 e with an average fluctuation of 0.057 e, for the two lines model the average charge is 4.430 e and the fluctuations are smaller - 0.024 e. We observed that electronic charge transfer from the copper surface to the nanowires is lower and electronic charge transfer to oxygen atoms bonded with tungsten atoms is higher for the two lines model. Generally, tungsten atoms in the two lines model show a tendency to have a decrease in their electron density compared with the one line model, although the difference is negligible. To consider the possible effect of these results on the position of photoemission lines we can compare them with values of charge calculated for a tungsten atom in bulk oxides, which is 4.654 e for monoclinic WO_3 and 2.971 e for rutile WO_2. The charge of the tungsten in our models is slightly lower but still closer to the value for the bulk W^{6+} than bulk W^{4+} ions. Thus we can assume that tungsten atoms in the observed tungsten oxide nanowires possess the W^{6+} oxidation state and the measured shift in the position of the W 4f core line originates from the reduced dimensionality of the structure.

In order to analyze the electronic structure, projected density of states (PDOS) curves were computed. PDOS of a tungsten atom is shown in Fig. 5(e)). It exhibits two bands below the Fermi level and these are shifted to lower energies in the case of the two lines model. The shape of the higher energy band for the two lines model resembles the shape of the bulk WO_3 PDOS curve more closely than the one line model. In case of PDOS of oxygen atoms shown in Fig. 5(f) two kinds of oxygen atoms were considered: laterally bonded oxygen $O_{lateral}$ and oxygen atom above the tungsten atom O_{above}. There are two oxygen bands below the Fermi level and again for

the two lines model these bands are shifted to lower energies. Due to these shifts we can conclude that the two lines model corresponds to a configuration that is more stable.

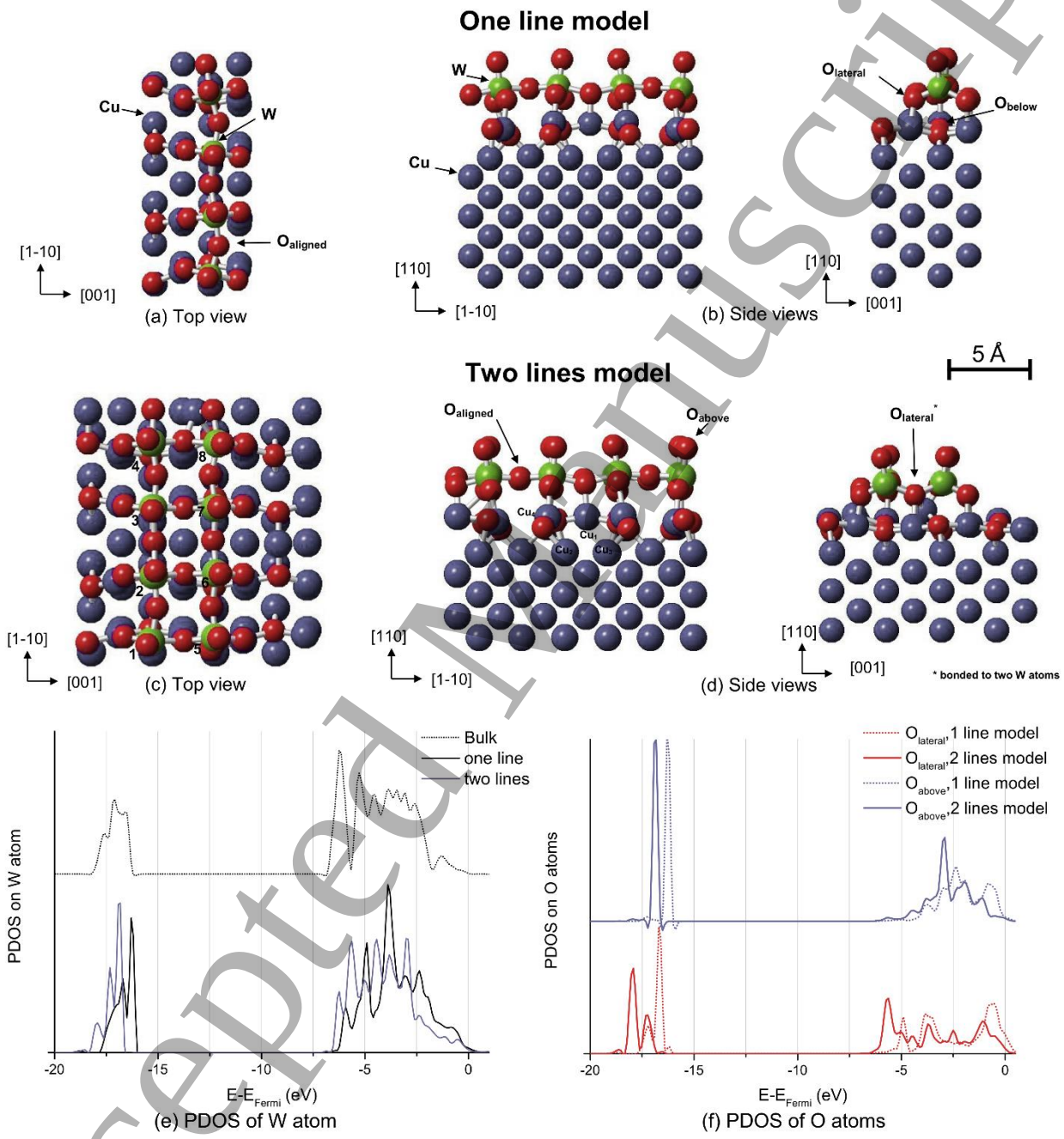

Figure 5. The lowest energy structures calculated by DFT: one line model (a), (b) and two lines model (c), (d) (Cu - blue, O - red, W - green). PDOS curves for different W (e) and O atoms (f).

Simulated STM images (Fig. 6(a) and (c)) obtained forboth models represent electron states from -1 eV up to the Fermi energy. A value of the constant charge density corresponding to a height of 6 Å above the surface was used. Comparing the calculated STM images for the one line and two lines models with experimental STM image (Fig. 6(b)) we can propose that both the one line and two lines features are present on the surface, alternating with oxidized Cu(110) surface exhibiting the c(6x2)-O reconstruction. One line features and c(6x2)-O like regions in between them exhibit the double periodicity of 7.66 Å along Cu[1-10] direction (Fig. 2(g), bottom profile). This interpretation supports our hypothesis based on the shape of calculated structures that the one line model represents the areas with double periodicity. Two lines features exhibit the single periodicity of 3.83 Å along Cu[1-10] direction (Fig. 2(g), top profile). One line features are appearing in pairs bordering the c(6x2)-O like regions which is clearly reflected by height profiles taken in Cu[001] direction in Fig. 2(h). Two lines features are also appearing in pairs approximately 7 Å apart (Fig. 2(i)). Linear protrusions or depressions along Cu[1-10] direction that separate the one line and two lines regions or two lines and two lines regions remain unidentified. These can be related to the rearrangement of the Cu(110) substrate (Fig. 2(a)) and represent Cu adatom rows on the Cu(110) substrate separating the tungsten oxide nanowires.

Figure 6. Simulated STM images of one line model (a) and two lines model (c) compared with experimental results (b) where the corresponding areas are marked by matching colors.

Origin of the formation of one-dimensional structures presumably lies in the Cu(110)-c(6x2)-O reconstruction of the surface since it is the most prominent difference between our experiment and the one carried out by Denk et al. [16]. They deposited WO_3 on the Cu(110)-(2x1)-O surface at low temperature (< 100 K) and after heating up to 600 K they obtained two-dimensional copper tungstenate. Closer inspection of our DFT models also supports this proposal because the nanowires grow directly on top of the oxygen atoms of the Cu(110)-c(6x2)-O reconstruction.

Conclusions

We have demonstrated the ability to prepare tungsten oxide model system by thermal evaporation of tungsten trioxide powder in highly reactive atmosphere of atomic oxygen. The obtained epitaxial tungsten oxide nanowires were comprehensively characterized by the means of experimental surface science and DFT calculations. One-dimensionality of the system was confirmed by RHEED, LEED, STM and DFT study of the structure. We identified unique electronic effects related to the system´s one-dimensionality – loss of dispersive valence band features in the direction perpendicular to the structures and chemical shift of the W 4f core emission line, which was clarified by the results of DFT calculations.

The characterized system can be used as an exemplary inverse model system for investigations of chemical properties and surface reactivity, e.g. in the NO_2 sensing applications of copper-doped tungsten oxide [39], or it can serve as a template for self-organized growth of novel one-dimensional systems.

AUTHOR INFORMATION

Corresponding Author

* E-mail: romana.tikka@gmail.com

Present Addresses

§ Peter-Grünberg-Institut 6, Forschungszentrum Jülich, GmbH, 52425 Jülich, Germany

§§ Johannes Kepler University Linz, Solid State Physics Division, Altenbergerstrasse 69, 4040 Linz, Austria

ACKNOWLEDGMENT

Presented research was supported by Vakuum Praha under the grant for 2016, Czech Science Foundation under the project GAČR 15-06759S, The Ministry of Education, Youth and Sports under the project MINCyT-MEYS ARC/13/11, UNS under the project SGCyT-UNS PGI 24/F128 and AGENCIA under the project PICT 2014-1351. C. P. and M. E. P. are members of CONICET. R. Š. also thanks Marie Aulická for her valuable help with ARPES measurement.

REFERENCES

[1] Netzer F P 2010 “Small and beautiful” - The novel structures and phases of nano-oxides *Surf. Sci.* **604** 485–9

[2] Kim C, Matsuura A Y, Shen Z X, Motoyama N, Eisaki H, Uchida S, Tohyama T and Maekawa S 1996 Observation of Spin-Charge Separation in One-Dimensional SrCuO2 *Phys. Rev. Lett.* **77** 4054–7

[3] Kobayashi K, Mizokawa T, Fujimori A, Isobe M and Ueda Y 1998 Single-Particle Excitations in One-Dimensional Mott-Hubbard Insulator NaV2O5 *Phys. Rev. Lett.* **80** 3121–4

[4] Netzer F P, Allegretti F and Surnev S 2010 Low-dimensional oxide nanostructures on metals: Hybrid systems with novel properties *J. Vac. Sci. Technol. B Microelectron.*

Nanom. Struct. **28** 1

[5] Rodriguez J A, Liu P, Graciani J, Senanayake S D, Grinter D C, Stacchiola D, Hrbek J and Fernández-Sanz J 2016 Inverse Oxide/Metal Catalysts in Fundamental Studies and Practical Applications: A Perspective of Recent Developments *J. Phys. Chem. Lett.* **7** 2627–39

[6] Solis J ., Saukko S, Kish L, Granqvist C . and Lantto V 2001 Semiconductor gas sensors based on nanostructured tungsten oxide *Thin Solid Films* **391** 255–60

[7] Abe R, Takami H, Murakami N and Ohtani B 2008 Pristine simple oxides as visible light driven photocatalysts: Highly efficient decomposition of organic compounds over platinum-loaded tungsten oxide *J. Am. Chem. Soc.* **130** 7780–1

[8] Wickman B, Wesselmark M, Lagergren C and Lindbergh G 2011 Tungsten oxide in polymer electrolyte fuel cell electrodes - A thin-film model electrode study *Electrochim. Acta* **56** 9496–503

[9] Tokarz-Sobieraj R, Hermann K, Witko M, Blume A, Mestl G and Schlögl R 2001 Properties of oxygen sites at the MoO3(010) surface: Density functional theory cluster studies and photoemission experiments *Surf. Sci.* **489** 107–25

[10] Gillet M, Lemire C, Gillet E and Aguir K 2003 The role of surface oxygen vacancies upon WO3 conductivity *Surf. Sci.* **532–535** 519–25

[11] Wang F, Di Valentin C and Pacchioni G 2011 Semiconductor-to-metal transition in WO3-x: Nature of the oxygen vacancy *Phys. Rev. B - Condens. Matter Mater. Phys.* **84** 1–

5

[12] Gillet M, Delamare R and Gillet E 2007 Growth, structure and electrical conduction of WO3 nanorods *Appl. Surf. Sci.* **254** 270–3

[13] Gillet M, Masek K, Potin V, Bruyère S, Domenichini B, Bourgeois S, Gillet E and Matolin V 2008 An epitaxial hexagonal tungsten bronze as precursor for WO3 nanorods on mica *J. Cryst. Growth* **310** 3318–24

[14] Kim H, Senthil K and Yong K 2010 Photoelectrochemical and photocatalytic properties of tungsten oxide nanorods grown by thermal evaporation *Mater. Chem. Phys.* **120** 452–5

[15] Li Z, Zhang Z, Kim Y K, Smith R S, Netzer F, Kay B D, Rousseau R and Dohnálek Z 2011 Growth of ordered ultrathin tungsten oxide films on pt(111) *J. Phys. Chem. C* **115** 5773–83

[16] Denk M, Kuhness D, Wagner M, Surnev S, Negreiros F R, Sementa L, Barcaro G, Vobornik I, Fortunelli A and Netzer F P 2014 Metal tungstates at the ultimate two-dimensional limit: Fabrication of a CuWO4 nanophase *ACS Nano* **8** 3947–54

[17] Hansen P L, Wagner J B, Helveg S, Rostrup-Nielsen J R, Clausen B S and Topsøe H 2002 Atom-resolved imaging of dynamic shape changes in supported copper nanocrystals. *Science* **295** 2053–5

[18] Andryushechkin B V., Cherkez V V., Pavlova T V., Zhidomirov G M and Eltsov K N 2013 Structural transformations of Cu(110) surface induced by adsorption of molecular chlorine *Surf. Sci.* **608** 135–45

[19] Aulická M, Duchoň T, Dvořák F, Stetsovych V, Beran J, Veltruská K, Mysliveček J, Mašek K and Matolín V 2015 Faceting transition at the oxide - Metal Interface: (13 13 1) facets on Cu(110) induced by carpet-like ceria overlayer *J. Phys. Chem. C* **119** 1851–8

[20] Ma L, Doudin N, Surnev S, Barcaro G, Sementa L, Fortunelli A and Netzer F P 2016 Lattice Strain Defects in a Ceria Nanolayer *J. Phys. Chem. Lett.* **7** 1303–9

[21] Kern K, Niehus H, Schatz A, Zeppenfeld P, Goerge J and Comsa G 1991 Long-range spatial self-organization in the adsorbate-induced restructuring of surfaces: Cu{100}-(2×1)O *Phys. Rev. Lett.* **67** 855–8

[22] Qin Y, Hua D and Li X 2013 First principles study on the surface- and orientation-dependent electronic structure of a WO 3 nanowire *J. Semicond.* **34** 062002

[23] Šedivá R, Mašek K, Pronsato M E and Pistonesi C 2016 Tungsten oxide nanowire on copper surfaces: a DFT model *RSC Adv.* **6** 88463–8

[24] Qin Y and Ye Z 2016 DFT study on interaction of NO2 with the vacancy-defected WO3 nanowires for gas-sensing *Sensors Actuators B Chem.* **222** 499–507

[25] Tanuma S, Powell C J and Penn D R 1993 Calculations of electron inelastic mean free paths (IMFPS). IV. Evaluation of calculated IMFPs and of the predictive IMFP formula TPP-□ 2 for electron energies between*Surf. Interface Anal.* **20** 77–89

[26] Kresse G and Hafner J 1993 Ab initio molecular dynamics for open-shell transition metals *Phys. Rev. B* **48** 13115–8

[27] Kresse G and Hafner J 1994 Ab initio molecular-dynamics simulation of the liquid-

metal–amorphous-semiconductor transition in germanium *Phys. Rev. B* **49** 14251–69

[28] Kresse G and Furthmüller J 1996 Efficient iterative schemes for ab initio total-energy calculations using a plane-wave basis set *Phys. Rev. B* **54** 11169–86

[29] Kresse G and Joubert D 1999 From ultrasoft pseudopotentials to the projector augmented-wave method *Phys. Rev. B* **59** 1758–75

[30] Perdew J P, Burke K and Ernzerhof M 1996 Generalized Gradient Approximation Made Simple. *Phys. Rev. Lett.* **77** 3865–8

[31] Perdew J P, Burke K and Ernzerhof M 1997 Generalized Gradient Approximation Made Simple *Phys. Rev. Lett.* **78** 1396

[32] Tang W, Sanville E and Henkelman G 2009 A grid-based Bader analysis algorithm without lattice bias. *J. Phys. Condens. Matter* **21** 084204

[33] Kishimoto S, Kageshima M, Naitoh Y, Li Y J and Sugawara Y 2008 Study of oxidized Cu(110) surface using noncontact atomic force microscopy *Surf. Sci.* **602** 2175–82

[34] Ichimiya A and Cohen P I 2004 Reflection High Energy Electron Diffraction (Cambridge University Press) pp 103–7

[35] Gillet M, Mašek K and Gillet E 2004 Structure of tungsten oxide nanoclusters *Surf. Sci.* **566–568** 383–9

[36] Mašek K, Libra J, Skála T, Cabala M, Matolín V, Cháb V and Prince K C 2006 SRPES investigation of tungsten oxide in different oxidation states *Surf. Sci.* **600** 1624–7

[37] Diehl R, Brandt G and Salje E 1978 The crystal structure of triclinic WO3 *Acta Cryst. B* **34** 1105–11

[38] Loopstra B O and Rietveld H M 1969 Further refinement of the structure of WO3 *Acta Cryst. B* **25** 1420–1

[39] Rossinyol E, Prim A, Pellicer E, Rodríguez J, Peiró F, Cornet A, Morante J R, Tian B, Bo T and Zhao D 2007 Mesostructured pure and copper-catalyzed tungsten oxide for NO2 detection *Sensors Actuators, B Chem.* **126** 18–23